CONDENSED MATTER: ELECTRONIC STRUCTURE, ELECTRICAL, MAGNETIC, AND OPTICAL PROPERTIES

Raman analysis of defects in n-type 4H-SiC

Vol 17 No 9, September 2008
1674-1056/2008/17(09)/3459-05

Chinese Physics B

Raman analysis of defects in n-type 4H-SiC*

Yang Yin-Tang(杨银堂)[a)†], Han Ru(韩　茹)[a)], and Wang-Ping(王　平)[b)]

[a)] *School of Microelectronics, Xidian University, Key Laboratory of Ministry of Education for Wide Band-Gap Semiconductor Materials and Devices, Xi'an* 710071, *China*
[b)] *Qimonda Technologies Xi'an, Xi'an* 710075, *China*

(Received 1 December 2007; revised manuscript received 17 April 2008)

This paper employs micro-Raman technique for detailed analysis of the defects (both inside and outside) in bulk 4H-SiC. The main peaks of the first-order Raman spectrum obtained in the centre of defect agree well with those of perfect bulk 4H-SiC, which indicate that there is no parasitic polytype in the round pit and the hexagonal defect. Four electronic Raman scattering peaks from nitrogen defect levels are observed in the round pit (395 cm^{-1}, 526 cm^{-1}, 572 cm^{-1}, and 635 cm^{-1}), but cannot be found in the spectra of hexagonal defect. The theoretical analysis of the longitudinal optical plasmon–phonon coupled mode line shape indicates the nonuniformity of nitrogen distribution between the hexagonal defect and the outer area in 4H-SiC. The second-order Raman features of the defects in bulk 4H-SiC are well-defined using the selection rules for second-order scattering in wurtzite structure and compared with that in the free defect zone.

Keywords: silicon carbide, electronic Raman scattering, round pit, hexagonal defect
PACC: 7280J, 3220F

1. Introduction

Silicon carbide is an attractive semiconductor for high power, high temperature, and high frequency electronic devices owing to its superior properties.[1] To meet the challenge of commercialization of SiC semiconductors, specific efforts have been made towards larger diameter high quality SiC bulk crystals. However, there are still various defects in SiC crystals that have to be eliminated, such as the round pits,[2] hexagonal defects,[3−5] micropipes,[3] stacking faults,[6] and polytype inclusion. These defects limit the performance and threaten the reliability of SiC-based devices. It has been concluded that the high density shallow growth pits with sharp tips could conceivably enhance the carrier emission/leakage in SiC Schottky diodes and degrade the MOS insulator reliability.[7] The research of Soloviev *et al* showed the correlation between oxide breakdown and defects in SiC wafers.[5]

Raman scattering is a non-destructive and contact-free technique which is used for the characterization of semiconductors. In 1972, Klein *et al* established a theory of plasmon–phonon coupling, which successfully predicted Raman line shapes for n-type nitrogen doped 6H-SiC.[8] Following Ref.[8], many researchers studied the electronic Raman scattering from nitrogen donor levels in other SiC polytypes.[9−11] However, reports on the electronic Raman scattering of defects in 4H-SiC and their second-order Raman spectra are quite few.

In this article, we report the Raman scattering data from the defects in bulk 4H-SiC which demonstrate that there is no parasitic polytypes in the round pit and the hexagonal defect. The electronic Raman scattering from nitrogen in hexagonal defect and its second-order Raman features are much different from that in free defect zone.

2. Experiment

The bulk 4H-SiC substrate (n-type, with a doping concentration of 2.5×10^{17} cm^{-3}) from SiCrystal AG company was employed in experiments presented in this paper. For the electronic Raman scattering analysis of bulk 4H-SiC, threefold (40, 70, 110 keV) implantation was carried out at 400°C to form a box profile (depth: 0.179 μm) of nitrogen (N) atoms with a mean concentration of 1.12×10^{19} cm^{-3}. The influence of N ions at each implantation energy was determined by Monte Carlo simulation using transport of ions in matter. The doses for threefold ion implantation were 6.0×10^{13} cm^{-2}, 6.0×10^{13} cm^{-2}, and 8.0×10^{13} cm^{-2}. Then, the doses were activated in pure Ar atmosphere

*Project supported by the National Defense Pre-Research Foundation of China (Grant Nos 51308030201 and 51323040118).
†E-mail: ytyang@xidian.edu.cn

at 1600°C for 1 h, so, the final activated carrier concentration was $2.8 \times 10^{18}\,\mathrm{cm}^{-3}$.

The micro-Raman scattering experiments were carried out under Renishaw inVia Raman microscope at room temperature. The 514.5 nm line of a 20 mW Ar^+ laser was employed as the excitation source. A spectral scan was collected between $100\,\mathrm{cm}^{-1}$ and $2000\,\mathrm{cm}^{-1}$, and the accuracy of the frequency measurement was $\pm 1.0\,\mathrm{cm}^{-1}$.

3. Results and discussions

The defect structure of bulk SiC crystal is very complex. Typical SiC wafers contain dislocations, planar defects (triangular or polygonal), round pits, micropipes and so on. The study of Ferrero *et al*[12] shows that either bulk wafers or wafers with epitaxial layers present high concentration of micropipes, but only bulk wafers show planar defects. The shallow round pit density increases dramatically as the growth temperature increases.[13] Hexagonal defect, which is identified to be a planar defect due to its similarity to the one reported in Ref.[14], is formed by embedded obstacles. While, Thomas *et al*[15] have shown that the hexagonal defect is formed at the interface between the seed crystal and crucible cap. Figure 1 shows a top view of the round pit and the hexagonal defect in bulk 4H-SiC.

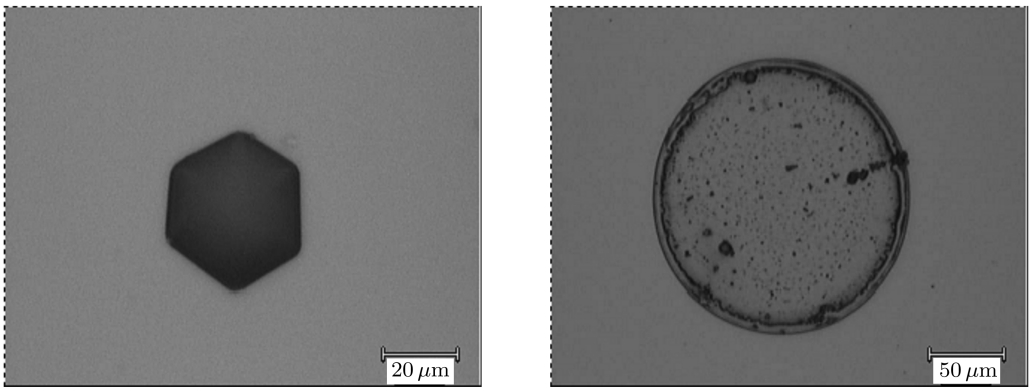

Fig.1. Hexagonal defect and round pit investigation by optical microscope.

3.1. Analysis of the first-order Raman spectra

The first-order Raman spectrum of SiC is polytype dependent, so it is very convenient to use Raman spectroscopy as a quick, very reliable method for polytype determination. The typical peaks in 4H-SiC Raman spectra are identifiable from previous studies.[16] Figure 2 shows the major peaks in the first-order Raman spectra from the centre of the defects and the outer area in 4H-SiC. It is clear that the intensity of the first-order Raman peaks is comparable between the round pit and the free defect zone. But the peaks of the hexagonal defect are less intense than that of the outer area. The major peaks in Fig.2 are an E_2 (TA: transverse acoustic) mode at $202.2\,\mathrm{cm}^{-1}$, an E_1 (TA) mode at $266.0\,\mathrm{cm}^{-1}$, an A_1 (LA: longitudinal acoustic) mode at $608.6\,\mathrm{cm}^{-1}$, an E_2 (TO: transverse optical) mode at $776.2\,\mathrm{cm}^{-1}$, an E_1 (LA) mode at $797.5\,\mathrm{cm}^{-1}$,

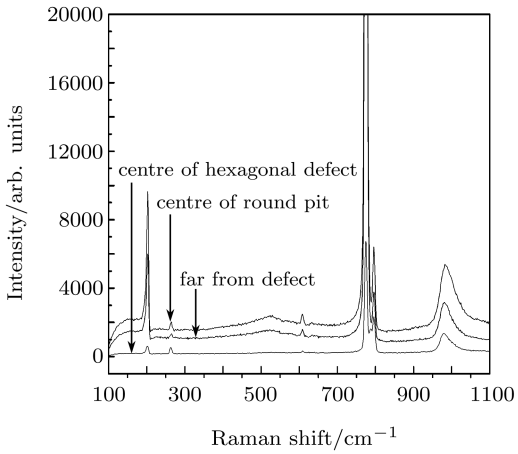

Fig.2. Raman spectra for n-type 4H-SiC taken at room temperature with excitation at 514.5 nm.

and an A_1 (LO: longitudinal optical) mode at about $985\,\mathrm{cm}^{-1}$. These peaks are evident in all the spectra of Fig.2 (inside or outside the defects), and agree well

with those of the perfect bulk 4H-SiC. This demonstrates that there are no parasitic polytypes in the round pit and the hexagonal defect of bulk 4H-SiC.

The carrier density n and mobility μ are deduced by analysing the line shape of LO plasmon–phonon coupled (LOPC) mode in Raman scattering.[17] The observed line shape of the LOPC mode is analysed by fitting the theoretical curve equation using a modified classical dielectric function (m-CDF) with ω_{p} (the plasma frequency), γ (the carrier damping), Γ_{L} (damping constant of the LO phonon) as adjustable parameters.[18] The carrier density n and mobility μ are derived from the best fit parameters of ω_{p} and γ using equations: $\omega_{\mathrm{p}}^2 = (4\pi nq^2)/(\varepsilon_\infty m^*)$; $\mu = q/(m^*\gamma)$. Where n, q and m^* are the density, charge, and effective mass of electron, respectively; ε_∞ is the optical dielectric constant. The values of n and μ in different areas are given in Fig.3. The lowest n and the highest μ are obtained in the centre of hexagonal defect. The carrier density n in the round pit approximately equal to that in free defect zone, but the μ in the round pit is the lowest one of the three.

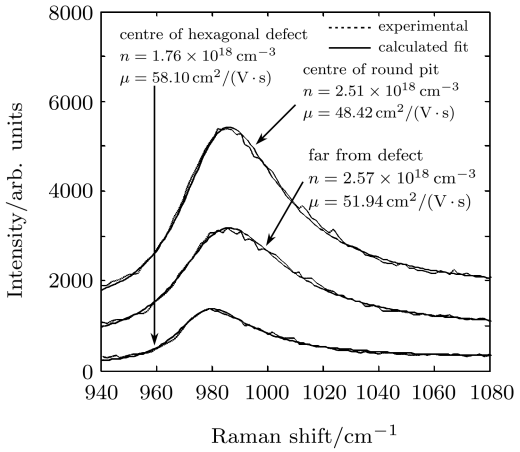

Fig.3. Experimental LOPC band (broken line) and calculated fit (solid line) for n-type bulk 4H-SiC.

3.2. Electronic Raman scattering from nitrogen doped 4H-SiC in round pit and hexagonal defect

In n-type SiC, nitrogen substitutes for carbon lattice. There exist two inequivalent C-lattice sites in 4H-SiC, which result in two different ionization energies depending on the position of nitrogen atom (on hexagonal lattice site or quasi-cubic lattice site).[19] The main features of donor bound exciton and donor bound multiexciton in indirect band gap semiconductors, like SiC, can be explained with Kirczenow's shell model.[20] The electronic Raman scattering can provide information about the 1s(A_1)-1s(E) valley-orbit (VO) splitting of the N_{c}-donor ground state.

Figure 4 shows the electronic Raman scattering from nitrogen in the centre of round pit and the hexagonal defect in 4H-SiC, the wave-number range is from 250 to 750 cm^{-1} (31 meV to 93 meV). The study of Burton and Long shows that,[11] when the excitation is in the red or near IR, clear resonant enhancements could be observed for three peaks in nitrogen-doped 4H-SiC (located at 400, 530 and 570 cm^{-1}, respectively). Because of the high donor concentration (about $1.12 \times 10^{19}\,\mathrm{cm}^{-3}$), the electronic Raman peaks associated with nitrogen could be observed with the excitation at 514.5 nm. At least four peaks at approximately 395 cm^{-1} (49 meV), 526 cm^{-1} (65.3 meV), 572 cm^{-1} (71 meV), and 635 cm^{-1} (78.8 meV), are enlarged and labelled N_{a}, N_{b}, N_{c} and N_{d} in the centre of round pit and the free defect zone. The peak N_{a} observed with excitation at 514.5 nm is weaker than that observed with excitation at 785 nm in Ref.[11], as the 785 nm excitation condition can enhance the electronic Raman scattering from nitrogen defect levels (the electronic energy levels of nitrogen donors) in 4H-SiC. The peaks at N_{a}, N_{b}, N_{c} are consistent with previous measurements of n-type 4H-SiC.[11] N_{a} may be due to local vibrational mode of nitrogen atom, while N_{b} and N_{c} are assigned to the VO splitting of the ground state at the k (quasi-cubic) site in the 4H-SiC. N_{d} could be explained by the transitions at energetically deep places of malfunction.[21] The VO splitting for h (hexagonal) site in 4H-SiC is 7.1 meV.[10]

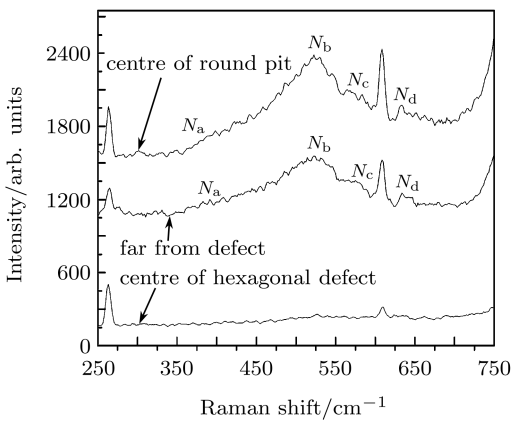

Fig.4. Electronic Raman scattering from nitrogen in the centre of round pit and hexagonal defect in 4H-SiC.

The four high frequency peaks and the low frequency mode at 57 cm^{-1} (7.1 meV) make for a total of four peaks that can be attributed to nitrogen donors in 4H-SiC.

It is clear from Fig.4 that, in different sample areas, the nitrogen electronic Raman spectra are different. There is no change in the major peaks between the spectra of the round pit and the free defect zone in 4H-SiC. From Fig.3, the value of n in free defect zone is almost the same as that in the round pit. This illustrates that the existence of round pit cannot affect the distribution of nitrogen concentration. But, the absence of peaks N_a, N_b, N_c and N_d in the centre of hexagonal defect demonstrates that the activated nitrogen concentration is lower than that in the free defect zone, which could easily find in Fig.3 (n in the free defect zone is approximately one-half times as large as that in the hexagonal defect.). The electronic Raman scattering in 4H-SiC is much sensitive to the activated nitrogen concentration. The existence of hexagonal defect is a serious limitation to the uniformity of nitrogen distribution in SiC wafer. It also restricts the performance of SiC-based device. Soloviev *et al*[5] show that the oxide breakdown under high fields is observed to occur at the edge of a hexagonal defect in SiC wafer, but no oxide breakdown is observed exactly above a micropipe. The triangular-shaped defects severely degrade high-blocking capability of the SiC diodes whereas shallow round pits give no direct impact.[2] Thus, the main reasonable result in breakdown is the nonuniformity of nitrogen distribution between the free defect zone and the hexagonal defect.

3.3. Second-order Raman scattering from the defects in bulk 4H-SiC

Figure 5 shows the second-order Raman scattering from different areas in bulk 4H-SiC. The spectrum in the centre of round pit is consistent with that in the free defect zone. According to the selection rules for second-order scattering in hexagonal materials,[22] the experimental Raman features at 1478 cm^{-1}, 1516 cm^{-1}, 1542 cm^{-1}, 1688 cm^{-1}, 1712 cm^{-1} and 1920 cm^{-1} (labelled a, b, c, d, e, and f) are assigned to two-phonon Raman scattering. Peak a is the overtone of the TO(K) at 737 cm^{-1}, b is the overtone of the TO(L) at 758 cm^{-1}, c is the overtone of the TO(M) at 771 cm^{-1}, d and e are the overtones of the LO(M) at 840 and 856 cm^{-1}, f is the overtone of the TO(Γ) at 965 cm^{-1}. The features at 1621 cm^{-1} and 1647 cm^{-1} (labelled g, h) are assigned to the combinations of phonons LO(K) and TO(K), also given in Ref.[23]. The theoretical calculation of the phonon dispersion curve in 4H-SiC[24] shows that the features at 1403 cm^{-1} and 1577 cm^{-1} (labelled i, j) can only formed by the combinations of phonons of acoustic mode and optical mode. In Fig.5, there are only six peaks (a, b, d, e, f and g) observed in the spectra from the centre of hexagonal defect. Skowronski and Ha[6] have investigated that the difference between the perfect crystal and the one containing the fault is the presence of a two-dimensional (2D) split-off band below the conduction band. In view of the 2D split-off band and the absence of the second-order Raman peaks c and h, the existence of hexagonal defect must affect the M point and K point phonon dispersion in this area. However, it is unclear how the hexagonal defect of the sample affects the dispersion of the phonon.

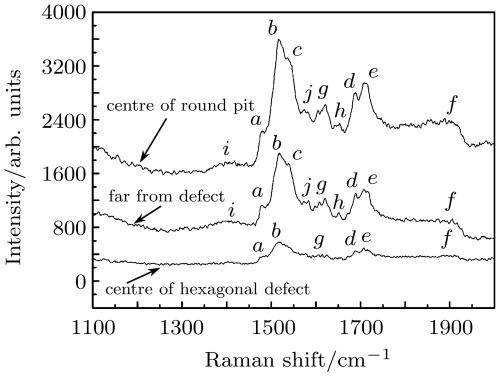

Fig.5. Second-order Raman scattering in the defect of 4H-SiC.

4. Conclusions

Micro-Raman spectra were measured for the defects on the bulk 4H-SiC wafer. In the centre of the round pit and the hexagonal defect, the main peaks of the Raman spectrum agree well with those of perfect bulk 4H-SiC. This indicates that there is no parasitic polytype in the round pit and the hexagonal defect. However, the existence of hexagonal defect restricts the uniformity of the distribution of nitrogen in 4H-SiC whereas the round pit gives little impact. The theoretical analysis of the LOPC mode line shape demonstrates the nonuniformity of nitrogen distribu-

tion between the hexagonal defect and the outer area in 4H-SiC. There are four electronic Raman scattering peaks from nitrogen defect levels, which are observed in the round pit ($395\,\mathrm{cm}^{-1}$, $526\,\mathrm{cm}^{-1}$, $572\,\mathrm{cm}^{-1}$, and $635\,\mathrm{cm}^{-1}$), but cannot be found in the spectra of hexagonal defect. The nonuniformity of nitrogen distribution is the main reason for the poor performance of SiC based devices. The second-order Raman features of the defects in bulk 4H-SiC are well-defined and compared with that in the free defect zone.

References

[1] Guo H, Zhang Y M and Zhang Y M 2007 *Chin. Phys.* **16** 1573

[2] Kimoto T, Miyamoto N and Matsunami H 1999 *IEEE Trans. Electron Devices* **46** 471

[3] Han R J, Xu X G, Hu X B, Naisen Yu, Wang J Y, Tian Y L and Huang W X 2003 *Opt. Mater.* **23** 415

[4] Syvajarvi M, Ciechonski R R, Yazdi G R and Yakimova R 2005 *J. Cryst. Growth* **275** e1103

[5] Soloviev S, Khlebnikov I, Madangarli V and Sudarshan T S 1998 *J. Electron. Mater.* **27** 1124

[6] Skowronski M and Ha S 2006 *J. Appl. Phys.* **99** 011101

[7] Ma X Y, Chang H, Zhang Q C and Sudarshan T 2005 *J. Cryst. Growth* **279** 425

[8] Klein M V, Ganguly B N and Colwell P J 1972 *Phys. Rev.* B **6** 2380

[9] Gorban I S, Gubanov V A, Kulakovskii V D, Skirda A S and Shepel B N 1988 *Sov. Phys. Semicond.* **30** 928

[10] Nakashima S and Harima H 1997 *Phys. Status Solidi* A **162** 39

[11] Burton J C and Long F H 1999 *J. Appl. Phys.* **86** 2073

[12] Ferrero S, Porro S and Giorgis F 2002 *J. Phys.*: *Condens. Matter* **14** 13397

[13] Chen W Z, Lee K and Capano M A 2006 *J. Cryst. Growth* **297** 265

[14] Nishino S 1995 *J. Cryst. Growth* **147** 339

[15] Thomas A K, Edward K S and Marek S 2001 *J. Appl. Phys.* **8**9 4625

[16] Ashraf H 2005 *Investigation of Symmetries of Phonons in 4H and 6H-SiC by Infrared Absorption and Raman Spectroscopy* MSc thesis at Linköping University, Sweden

[17] Chafai M, Jaouhari A, Torres A, Anton R, Martin E, Jimenez J and Mitchel W C 2001 *J. Appl. Phys.* **90** 5211

[18] Nakashima S, Harima H, Ohtani N and Katsuno M 2004 *J. Appl. Phys.* **95** 3547

[19] Pernot J, Zawadzki M, Contreras S, Robert J L, Neyret E and Cioccio L D 2001 *J. Appl. Phys.* **90** 1869

[20] Kirczenow G 1977 *Solid State Commun.* **21** 713

[21] Gerstmann U, Rauls E, Frauenheim T and Overhof H 2003 *Phys. Rev.* B **67** 205202

[22] Gorban I S and Lugovoi V I 1976 *Zh. Prikl. Spektrosk.* **24** 333

[23] Gao X, Sun G S, Li J M, Wang L, Zhan W S and Zhang Y M 2004 *Chin. J. Semiconductors* **25** 1555

[24] Hofmann M, Zywietz A, Karch K and Bechstedt F 1994 *Phys. Rev.* B **50** 13401